

Designing a Corrosion Health Monitoring System

Danny L. Parker¹, and Philip Dussault²

¹AVNIK Defense, Huntsville, AL, 35801, USA

dparker@avnikdefense.com

²AMRDEC, Redstone Arsenal, AL, 35806, USA

Philip.L.Dussault.civ@mail.mil

ABSTRACT

This paper demonstrates the ability to design health monitoring systems from a systematic perspective and, with proper sensor and actuator placement, to detect and track corrosion occurring in a structure. The results from two sample coupons are presented showing the daily progression of corrosion. The tests were performed and the data were collected to emulate on-ground health monitoring scenarios where the vehicle or structure under test is at rest. The data show a strong correlation between the amount of corrosion and the calculated damage metric.

To achieve these results, a design optimization was performed to determine the best locations to excite the structure and to collect data while using the minimum number of sensors. The techniques used to design the monitoring system allow for any type of sensor (thermal, strain, electromagnetic, etc.) and can find the optimal locations with respect to defined objective functions (sensitivity, cost, etc.). They also account for modeling error and variations in boundary conditions. The use of model-based optimization techniques for the design of the monitoring system is driven by the desire to obtain the best performance possible from the system given what is known about the system prior to implementation. The use of a model is more systematic than human judgment and is able to take far more into account concerning the dynamical response of a system than even an experienced structural engineer.

1. SYSTEM DESIGN

Corrosion can be a major cost driver for maintaining equipment. Currently, in order to detect the existence of corrosion in a component / structure, visual inspections are typically done on a scheduled basis. The disassembly and inspection of a component can be a labor intensive process

that is sometimes unnecessary because no damage developed during the inspection interval. In general, maintainers would like to move from a costly interval inspection based paradigm to one of condition based maintenance (CBM). A CBM system's goal is to determine the equipment's health and to initiate inspections only when maintenance is actually necessary thus minimizing spare parts cost, system downtime and overall time spent on maintenance.

The purpose of the test was to demonstrate the ability to design health monitoring systems from a systematic perspective and, with proper sensor and actuator placement, to detect and track damage occurring in a structure. To this end, a design optimization was performed to determine the best locations to excite the structure and to collect data while using the minimum number of sensors using methods introduced by (Frazier, Parker, and Rinehart, 2004) and more fully explored in (Parker 2011). The type of sensors used in this case was a uni-axis accelerometer. It should be noted that the design algorithms used here are not limited to accelerometers. They allow for any type of sensor (thermal, strain, electromagnetic, etc.) as long as mathematical models are provided and find the optimal locations with respect to user-defined objective functions (sensitivity, cost, etc.) (Parker, Frazier, Rinehart & Cuevas 2006). The use of model-based optimization techniques for the design of the monitoring system is driven by the desire to obtain the best performance possible from the system given what is known about the system prior to implementation. The use of a model is more systematic than human judgment and is able to take far more into account concerning the dynamical response of a system than even an experienced structural engineer. It is understood in the context of structural modeling that all models have errors and that good designs produced by model-based techniques should be tolerant to these errors. Demonstrations performed in the past have shown that poorly placed sensors can be very insensitive to damage development (Frazier & Parker 2003).

Danny Parker et al. This is an open-access article distributed under the terms of the Creative Commons Attribution 3.0 United States License, which permits unrestricted use, distribution, and reproduction in any medium, provided the original author and source are credited.

A multi-objective genetic algorithm (GA) was employed to perform the optimization. The foundations of this method are presented in (Rinehart 2005). The objectives of the optimization were to maintain adequate ability to detect damage occurring elsewhere in the structure and maintain robustness to modeling errors. A third objective was to minimize the number of sensors and actuators used.

Because of the size of the search space and the computational costs associated with evaluating the objective functions, the GA was implemented on a 16-core parallel computing cluster. Each individual in the population of the GA was evaluated on its own core and the total optimization time was approximately 3 weeks. When the GA completed it produced a set of optimal designs using 2 to 6 sensors and 1 or 2 actuators. These designs were simulated (time-domain) to assess their performance. The simulations tested the design's sensitivity to damage occurring random locations. Figure 1 shows the sensitivity of each possible sensor location to damage occurring on the plate where the red areas have a higher sensitivity. A 3-sensor and 1-actuator design was chosen to implement in the salt fog test.

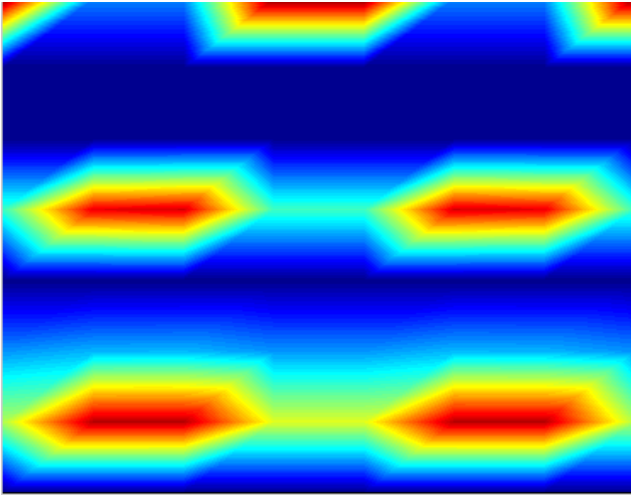


Figure 1. Sensitivity of a Simple Plate

The sensor-actuator layout is shown in Figure 2 with the appropriate dimensions given in Table 1. For further information about the optimal design techniques used here the reader is referred (Rinehart 2005), (Frazier et al. 2004), (Parker 2011), and (Cuevas, Parker, Frazier, & Weatherford 2008).

Table 1. Sensor and Actuator Locations

Device	Length (mm)	Width (mm)
P1	63.5	41.275
A1	41.275	22.225
A2	44.45	53.975
A3	95.25	57.15

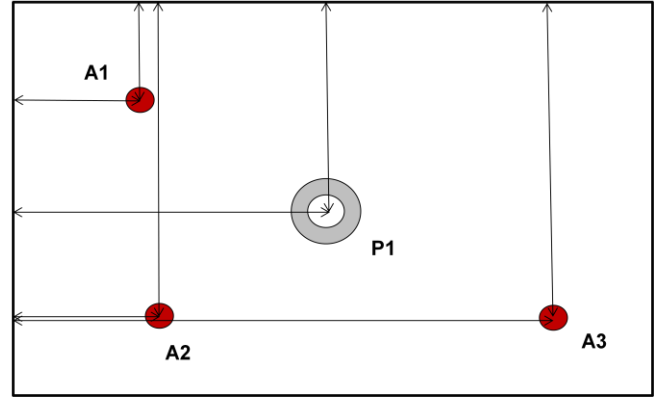


Figure 2. Sensor Layout

2. DESIGN PROCESS OVERVIEW

Assume that the physical phenomena (elastic, thermal, electromagnetic, etc.) of interest for the structure can be modeled adequately as a LTI dynamical system in state-space form; i.e.,

$$\begin{aligned}\dot{x}(t) &= Ax(t) + Bu(t) \\ y(t) &= Cx(t) + Du(t), \\ x(0) &= x_0\end{aligned}\quad (1)$$

where $x(t) \in R^n$ is the state vector, $u(t) \in R^m$ is the actuator signal vector, $y(t) \in R^p$ is the sensor signal vector, and $x_0 \in R^n$ is the initial state condition. The matrices $A \in R^{n \times n}$, $B \in R^{n \times m}$, $C \in R^{p \times n}$, and $D \in R^{p \times p}$ represent the system dynamics, actuator influence, sensor coupling, and direct feed through effects, respectively. Here, the symbols R^n and $R^{n \times m}$ are used to represent the spaces of n -dimensional real vectors and n -by- m real matrices, respectively. While this model framework may seem restrictive at first, it should be recalled that linear elastic finite-element methods (FEM) and finite-difference (FD) heat transfer modeling can be represented by this form quite easily.

To highlight a particular case, consider the familiar second-order vector form resulting from the application of FEM to an elastic structure:

$$M\ddot{z}(t) + G\dot{z}(t) + Kz(t) = Fu(t) \quad (2)$$

where M , G , and K , are the mass, damping, and stiffness matrices, respectively. Here, the matrix F maps the actuator signals into the usual force vector and should be thought of as specifying where independent forces are applied to the structure. The vector z consists of the translational and rotational degrees-of-freedom (DOF's). Using the definition

$$x = \begin{bmatrix} z \\ \dot{z} \end{bmatrix},$$

it is easy to see that

$$A = \begin{bmatrix} 0 & I \\ -M^{-1}K & -M^{-1}G \end{bmatrix}, B = \begin{bmatrix} 0 \\ M^{-1}F \end{bmatrix} \quad (3)$$

In the case where accelerometers are used for sensing,

$$y(t) = -C_a M^{-1} [K \ G] x(t) + C_a M^{-1} F u(t) \quad (4)$$

where C_a is a matrix specifying the locations of the accelerometers. This implies that $C = -C_a M^{-1} [K \ G]$ and $D = C_a M^{-1} F$. To be more precise, the structure of the matrix C_a is such that each row corresponds to the output of an accelerometer and each column corresponds to a DOF in the model.

Our goal in this work is to optimally position accelerometers on a structure to detect changes in the structure's dynamics assuming a known location for exciting the structure: i.e., we would like to determine the best matrix C_a . This corresponds to finding the best DOF's to measure. The excitation is chosen to be a zero-mean, Gaussian band-limited white noise with a covariance matrix Q_u . This introduces energy into all the modes of the system. The steady-state response of the system defined in Eq. (1) to this input is given by

$$Q_y = C Q_x C^T + D Q_u D^T \quad (5)$$

where Q_x is the steady-state covariance of the state vector x and can be shown to be the solution to the following matrix Lyapunov equation:

$$A Q_x + Q_x A^T + B Q_u B^T = 0 \quad (6)$$

Readily available numerical algorithms exist to solve Eq. (6). To optimally position the sensors it was decided to maximize the matrix 2-norm of the sensitivity of the steady-state sensor covariance Q_y with respect to parametric variations in the system matrices A , B , C , and D . To put this plainly, the algorithm tries to maximize the change in the output signal when damage develops in the structure. Recall, that in general, the entries of these matrices are determined by the geometry and physical properties of the materials used in the structure to be monitored. Other sensitivity measures are possible, but this one is sensitive to a large space of changes. It is given by

$$\begin{aligned} \frac{\partial Q_y}{\partial p} &= \frac{\partial C}{\partial p} Q_x C^T + C \frac{\partial Q_x}{\partial p} C^T + C Q_x \frac{\partial C^T}{\partial p} \\ &+ \frac{\partial D}{\partial p} Q_u D^T + D \frac{\partial Q_u}{\partial p} D^T + D Q_u \frac{\partial D^T}{\partial p} \end{aligned} \quad (7)$$

where $\frac{\partial Q_x}{\partial p}$ is the solution to

$$\begin{aligned} \frac{\partial A}{\partial p} Q_x + A \frac{\partial Q_x}{\partial p} + \frac{\partial Q_x}{\partial p} A^T + Q_x \frac{\partial A^T}{\partial p} \\ + \frac{\partial B}{\partial p} Q_u B^T + B Q_u \frac{\partial B^T}{\partial p} = 0 \end{aligned} \quad (8)$$

and p is a parameter characterizing the effect of damage on the structure. Usually p influences the entries of M , K , and G . Note that Eq. (8) is of the same form as Eq. (6) in its unknown.

Using these equations, along with a finite-dimensional model of a structure, a combinatorial design optimization algorithm, such as a genetic algorithm, can be used to find the optimal locations of the sensors.

3. TEST SETUP

To test the system performance the two test coupons were placed in a salt fog chamber. The test was configured to collect data every two minutes over the 69 hour test. The piezo actuator was driven with a 10 second sine chirp that went from 500 Hz to 10 kHz. The plates were tested independently meaning that the piezo one plate one was driven for 10 seconds, shut off, then the second plate was driven for the same amount of time.

In order to facilitate rapid completion of testing with accurate results, the spray scheduling of ASTM B117 was combined with the salt mixture from ASTM G85 annex 5. The constant spray and temperature (25°C) from B117 allowed us to have a steady controlled rate of corrosion. The salt mixture from ASTM G85-A5 is far more dilute and acidic than standard B117 salt solution. This created a rapid rate of corrosion while eliminating the possibility of salt crystals forming on the panels. A Q-FOG Cyclic Corrosion tester 1100 Liter salt fog chamber was used.

4. RESULTS

The primary optimization criterion we chose was the 2-norm of $\left\| \frac{\partial Q_y}{\partial p} \right\|_2$, which is a measure of the change in output power covariance in response to a structural parameter change (mass or stiffness reduction). In practice this quantity cannot be measured; however, for small changes in p , which is what we are after, it is clear that

$$\left\| \frac{\partial Q_y}{\partial p} \right\|_2 \propto \|Q_y^{ref} - Q_y^{dam}\|_2 \quad (9)$$

where Q_y^{ref} and Q_y^{dam} are the reference and damaged values of the output power covariance—quantities that can be measured. Thus the damage metric is represented as the change between a baseline and current covariance matrix.

While the experimental procedure was executed to correspond to the simulation studies, the test environment included many unmodeled events (sources of external ambient vibration, temperature variations, etc.). The data were filter to only include the frequencies between 700 Hz and 7 kHz.

The results of the salt fog test can be seen in Figure 3. One thing that immediately jumps out upon inspection is the large deviation on coupon 2 between 450 and 750 minutes. This was due to one sensor (A1) giving faulty readings during that time. It eventually corrected itself but no ultimate cause was discerned.

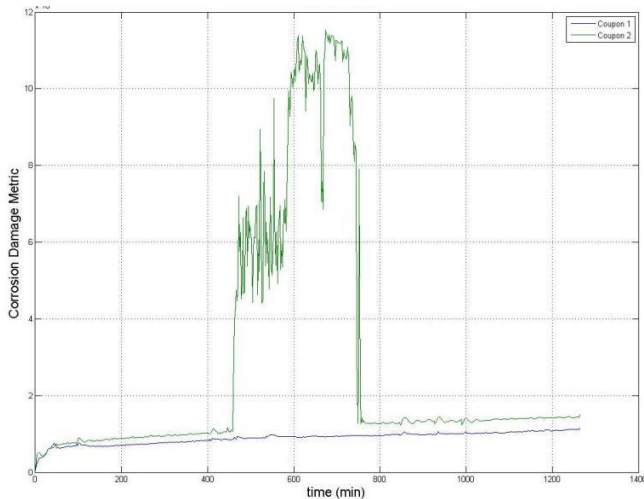


Figure 3. Three Sensor Results

To more clearly show the effects of the corrosion the data from both coupons were reprocessed with sensor A1 omitted. The results can be seen in Figure 4. A close up view of the first 80 minutes in the chamber is shown in Figure 5. Figure 6 shows the coupons after 69 hours in the salt fog chamber.

5. ANALYSIS OF RESULTS

The results in Figure 4 show a clear correlation between the amount of corrosion and the damage metric. A few things to note from the graph is there is initially a large change over the first 60 minutes. This was an unexpected result. While we designed the test to cause the coupons to corrode very fast so the total test time could be minimized, we still wanted to have some period of time before the corrosion could be detected by the system so a proper statistical baseline could be computed. The large initial change is partially due to the temperature changing for $\sim 23^\circ\text{C}$ to the test standard of 25°C . Rough thermodynamic calculations show that the coupons reach thermal steady-state in the first 12 minutes. The effects of this can be seen by the initial hump in Figure 5 that reaches a more steady process after 12 minutes. The rest of the response is due to the flash corrosion.

Some other features that are worth noting are the sharp spikes in Figure 4 that occur at approximately the 150, 400, 500, 550, 850, 950, and 1000 minute marks. These spikes are due to the salt fog chamber being opened so that pictures could be taken of the coupons at various stages of corrosion. This obviously illustrates the extreme sensitivity a system can possess when it has been designed optimally.

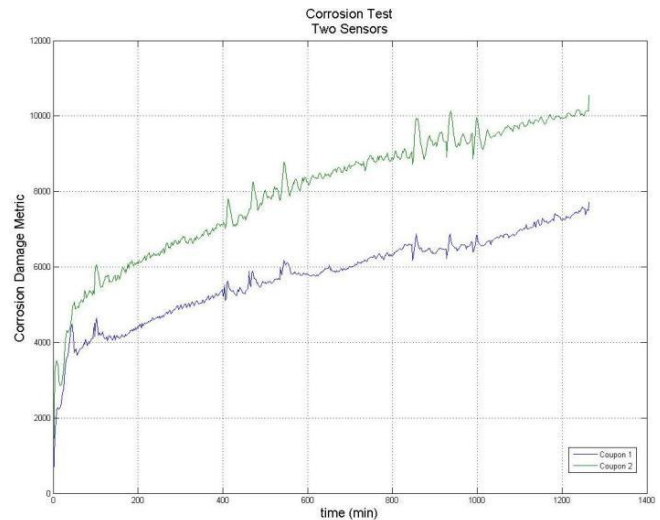


Figure 4. Two Sensor Results

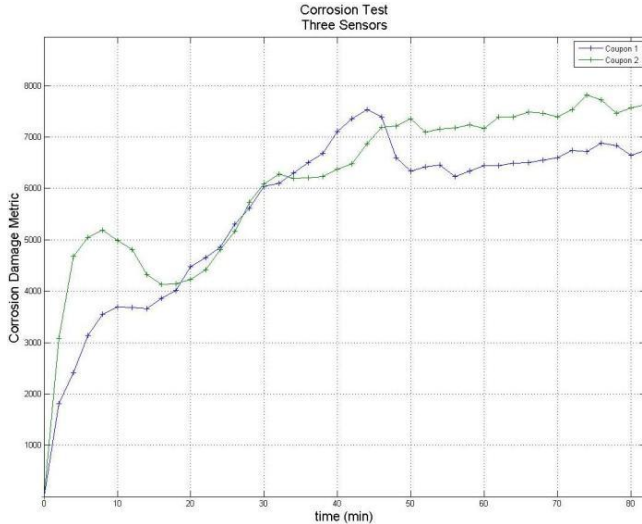


Figure 5. First 80 minutes of the Three Sensor System

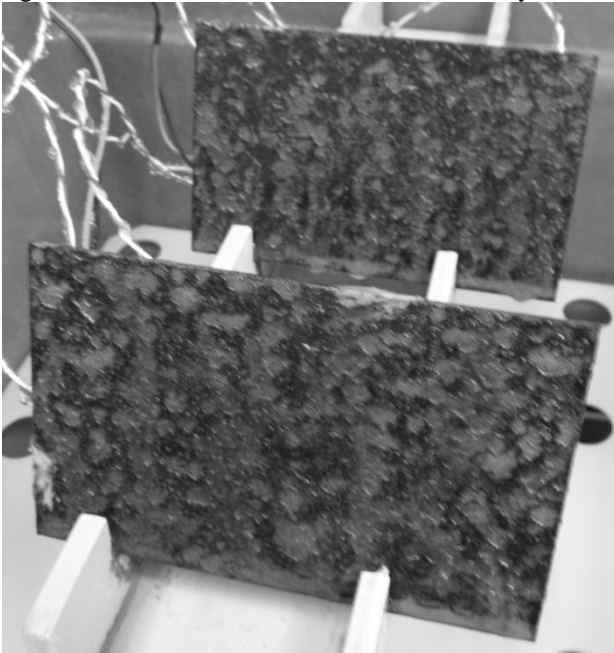


Figure 6. Coupons after 69 hours

6. CONCLUSION

This paper shows a systematic methodology for designing a health monitoring transducer configuration using dynamical system theory that is robust to modeling errors. The method produces designs that are highly sensitive to damage

developing in the structure. It was shown in the experiment that the damage metric was positively correlated to the increasing corrosion on the coupons. Clearly this demonstrates the potential of this methodology to provide early detection of damage development and is an essential first step in being able to predict the amount of corrosion into the future. It's not presented here but there has been significant work in compensating for environmental changes, such as temperature, to avoid false alarms in variable environments. This work will be presented at a future time.

Furthermore, new test are being carried out such that the lower limits of the amount of detectable corrosion can be established. This effort will establish a statistical baseline for an uncorroded coupon by better controlling the environmental aspects of the chamber.

REFERENCES

- Cuevas, P.S., Parker, D.L., Frazier, W.G., & Weatherford, D.D. (2008). Structural Damage Detection: A Study of Optimal Sensor Locations. *2nd Asia-Pacific Workshop on Structural Health Monitoring*, Melbourne, Australia.
- Frazier, W.G., & Parker, D.L. (2003). Dynamical Systems Research for Vehicle Health Monitoring. *AeroMat 2003*, Dayton, OH.
- Frazier, W.G., Parker, D.L., & Rinehart, H. (2004) A Dynamical Systems Engineering Approach to Vehicle Health Monitoring and Nondestructive Inspection System Design. *Proceedings of MS&T*, TMS Meeting, New Orleans, Sept 26-29, 2004.
- Parker, D.L., Frazier, W.G., Rinehart, H.S., & Cuevas, P.S. (2006). Experimental Validation of Optimal Sensor Placement Algorithms for Structural Health Monitoring. *Proceedings of the Third European Workshop on Structural Health Monitoring*, Grenada, Spain, July 5-7.
- Parker, D., (2011). *Multi-Objective Design Optimization Framework for Structural Health Monitoring*. Doctoral dissertation. Mississippi State University, Mississippi State, USA.
- Rinehart, H.S. (2005). *Model Based Optimal Design for Structural Health Monitoring*. Master's Thesis. University of Mississippi, Oxford, MS, USA.